Hindawi Publishing Corporation
Journal of Nanomaterials
Volume 2013, Article ID 712361, 7 pages
http://dx.doi.org/10.1155/2013/712361

Research Article

Self-Catalytic Growth of Tin Oxide Nanowires by Chemical Vapor Deposition Process

Bongani S. Thabethe,[1,2] Gerald F. Malgas,[1,2] David E. Motaung,[1] Thomas Malwela,[1] and Christopher J. Arendse[2]

[1] *DST/CSIR Nanotechnology Innovation Centre, National Centre for Nanostructured Materials, Council for Scientific and Industrial Research, P.O. Box 395, Pretoria 0001, South Africa*
[2] *Department of Physics, University of the Western Cape, Private Bag X17, Bellville 7535, South Africa*

Correspondence should be addressed to Gerald F. Malgas; gmalgas@csir.co.za and David E. Motaung; dmotaung@csir.co.za

Received 20 February 2013; Accepted 10 June 2013

Academic Editor: Rakesh Joshi

We report on the synthesis of tin oxide (SnO_2) nanowires by a chemical vapor deposition (CVD) process. Commercially bought SnO nanopowders were vaporized at 1050°C for 30 minutes with argon gas continuously passing through the system. The as-synthesized products were characterized using UV-visible absorption spectroscopy, X-ray diffraction (XRD), scanning electron microscopy (SEM), and high-resolution transmission electron microscopy (HRTEM). The band gap of the nanowires determined from UV-visible absorption was around 3.7 eV. The SEM micrographs revealed "wool-like" structure which contains nanoribbons and nanowires with liquid droplets at the tips. Nanowires typically have diameter in the range of 50–200 nm and length 10–100 μm. These nanowires followed the vapor-liquid-solid (VLS) growth mechanism.

1. Introduction

One-dimensional (1D) metal oxides semiconductor nanomaterials have attracted great interest as CO gas sensors due to their novel electronic and optical properties in nanodevices and because of their active sites to adsorb gas molecules and catalytic reactions [1–7]. These sensors play an essential role in the fields of industrial processing, environmental protection, and medical treatment. However, many problems need to be solved to further improve the selectivity, sensitivity, and stability of the sensors. Among them SnO_2, an n-type semiconductor with a wide direct band gap energy of 3.6 eV, is a particular material of interest because of its unique electrical properties, optical properties, small size, high sensitivity, good chemical stability, high electron mobility, fast response, and recovery speed [4, 8–10]. Tin oxide thin films find the best use in chemical sensors which are commercially available for detecting fuel gas, carbon monoxide, combustible gases, ammonia, water vapour, and numerous other gases and vapors [11].

Due to the enhanced surface-to-volume ratio of 1D structures, tin oxide nanowires have been shown to have excellent sensing performance which is comparable to or even better than the thin film sensors [12–14]. These structures with a high aspect ratio (i.e., size confinement in two coordinates) offer better crystallinity, higher integration density, and lower power consumption [15]. It has been reported by several authors that the performances of gas sensors can be enhanced by increasing the specific surface area by way of achieving nanoparticles [16, 17] and by incorporation of noble metals [18], such as platinum or gold. SnO_2 nanowires have been synthesized by different methods, such as laser ablation [19], solution [20], template-based method [21], chemical vapor deposition [22], and thermal evaporation [23]. In the last year, a great effort has been put into understanding and controlling the growth process for the preparation of high quality quasi one-dimensional nanostructures. In this study, we report on the self-catalytic growth of SnO_2 nanowires using a chemical vapor deposition process. The optical and structural

properties of the as-grown nanowires at room temperature are also studied.

2. Experimental Details

Tin oxide nanowires were grown on a silicon substrate and at the end of the tube by a CVD process using about one gram of monotin oxide (SnO) (purity 90%) at a growth temperature of 1050°C. The SnO was placed into a quartz boat and inserted into the centre of a quartz tube (radius = 5 cm, length = 20 cm) at a distance of about 1-2 cm from the Si substrate. The furnace temperature was increased from room temperature (25°C) to 1050°C for 30 min. The annealing was made in an argon atmosphere at atmospheric pressure. After cooling down, a fluffy layer of deposition could be collected from inside the tube wall ends in the lower end temperature zone or on the Silicon substrate.

UV-visible absorption measurements were carried out on the SnO nanopowders and the SnO_2 nanowires using a Perkin Elmer spectrophotometer in a range between 200 and 900 nm. The morphology of the product was examined by field-emission scanning electron microscopy (Auriga Zeiss SEM) with a beam energy of 3 keV. The crystal structure of the as-synthesized product was analysed by X-ray diffraction (XRD) analysis using a Phillips X-ray diffractometer. A high-resolution transmission electron microscope (HRTEM-JEOL-2000) was used to examine the internal structure of the as-synthesized product. The chemical compositions were determined using an energy dispersive X-ray spectrometer (EDS) attached to the HRTEM instrument.

3. Results and Discussion

The optical band gap of commercially bought SnO and SnO_2 nanowires was investigated using the UV-visible absorption spectrometer. Figure 1 shows the UV-vis spectra of the commercially bought SnO powder and as-synthesized SnO_2 nanowires at 1050°C for 30 min in argon gas. Both samples were dissolved in isopropanol for UV-vis analysis. A weak band edge absorption in the spectrum is observed around the 375 nm wavelength. The optical transition of SnO_2 crystals is known to be a direct type [24], where the absorption coefficient α can be expressed as [25]

$$(\alpha h\nu)^2 \propto \left(h\nu - E_g\right), \quad (1)$$

where $h\nu$ is the photon energy, E_g is the apparent optical band gap, and α is the absorption coefficient. Plots of $(\alpha h\nu)^2$ versus $h\nu$ can be derived from the absorption data in Figure 1 as shown in the inset. Therefore, the band gap can be obtained by extrapolation of the previous relation in the inset of Figure 1. The intercept of the tangent to the plot gives a good approximation of the band gap energy of direct band gap materials. The calculated energy band gap values are ~3.7 eV for SnO_2 nanowires and ~3.64 eV for commercially bought SnO powder, respectively. These values are slightly larger than that of bulk SnO_2 (3.62 eV) and might be due to the quantum size effect [26–28].

Table 1: Quantitative analysis of the SnO_2 nanowires.

Element	Atomic%	Weight%
O	64.53-	20.78-
Sn	30.42 ± 0.27	72.68 ± 0.64
Cu	2.71 ± 0.21	3.47 ± 0.27
Zn	2.33 ± 0.27	3.07 ± 0.36

Figure 2 shows the scanning electron microscopy (SEM) micrographs of Figure 2(a) commercially bought SnO powder and Figures 2(b) and 2(c) fluffy gray SnO_2 product that was collected on the wall of the inner quartz tube after it was synthesized at a growth temperature of 1050°C for 30 min. It is evident that the as-synthesized products are dominated by "wire-like" structures whose diameter varies from 50 to 200 nm. The length of the wires ranges from several tens to several hundred micrometers. Figures 3(a) and 3(b) show high magnification images of the nanowires. It is observed that spherical particles are attached to the ends of the nanowires. Energy-dispersive X-ray spectroscopy (EDS) analysis (Figure 4 and Table 1) extracted at four different spots showed that the tip of the nanowires consists of tin (Sn) and oxygen (O) only. The Cu and Zn peaks present in the EDS spectra are from the brass stubs used in the sample preparation. The result reveals that the products are the coexistence of Sn and O with a molar ratio of 33.21 : 66.64, which is consistent with the composition of SnO_2 and is in good agreement with the XRD results (Figure 5).

The X-ray diffraction analyses of the tin oxide precursor were carried out as shown in Figure 5(a). All the diffraction peaks can be attributed to the tetragonal tin oxide (SnO) (JCPDS 006-0395), with lattice constants of $a = b = 3.802$ Å and $c = 4.836$ Å. Figure 5(b) shows the X-ray diffraction pattern for the synthesized tin oxide nanowires and ribbons. From the diffraction patterns, the as-synthesized SnO_2 nanowires have a good crystallinity with the tetragonal tin oxide SnO_2 structure. The structure of the nanowires was further characterized by transmission electron microscopy and selected area electron diffraction (SAED) patterns. Figures 6(a) and 6(b) show a low and high magnification TEM image of a single SnO_2 nanowire, respectively, with uniform diameter. It is evident that the diameter of nanowires/nanobelts varies from 50 to 200 nm with a few Sn droplets on the nanowires. The observed tip morphology on top of the SnO_2 nanowires is consistent with the SEM analysis. The SAED pattern of the tip and the tail of the nanowires are shown in Figures 6(c) and 6(d), respectively. The patterns clearly confirm the polycrystalline nature of the nanowires. It should be pointed out that no metal catalyst was used during the growth of the nanowires. Therefore, based on these findings, we can conclude that the SnO_2 nanowires follow the vapor liquid-solid (VLS) growth mechanism.

The growth mechanism of nanowires in thermal evaporation [29] can be explained by either vapour-liquid-solid (VLS) [30] and or vapour-solid (VS) [31]. Vapor-liquid-solid (VLS) mechanism is a catalyst-assisted growth process, where metal nanoclusters or nanoparticles are used as the nucleation seeds. These nucleation seeds determine the interfacial

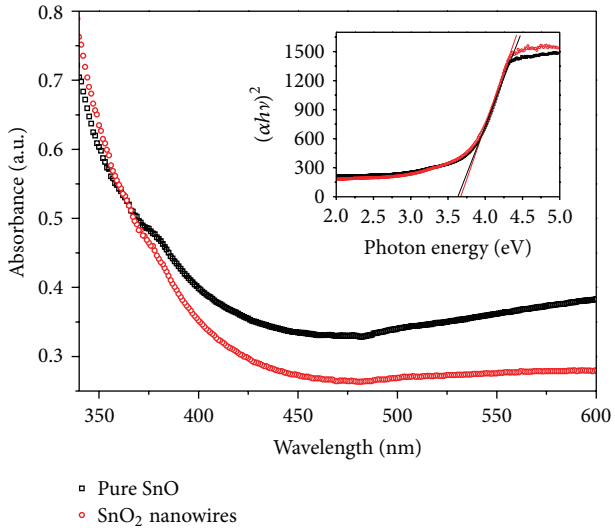

FIGURE 1: UV-visible absorption spectra of commercially bought SnO powder and SnO_2 nanowires. The inset shows the $(\alpha h\nu)^2$ versus photon energy curve.

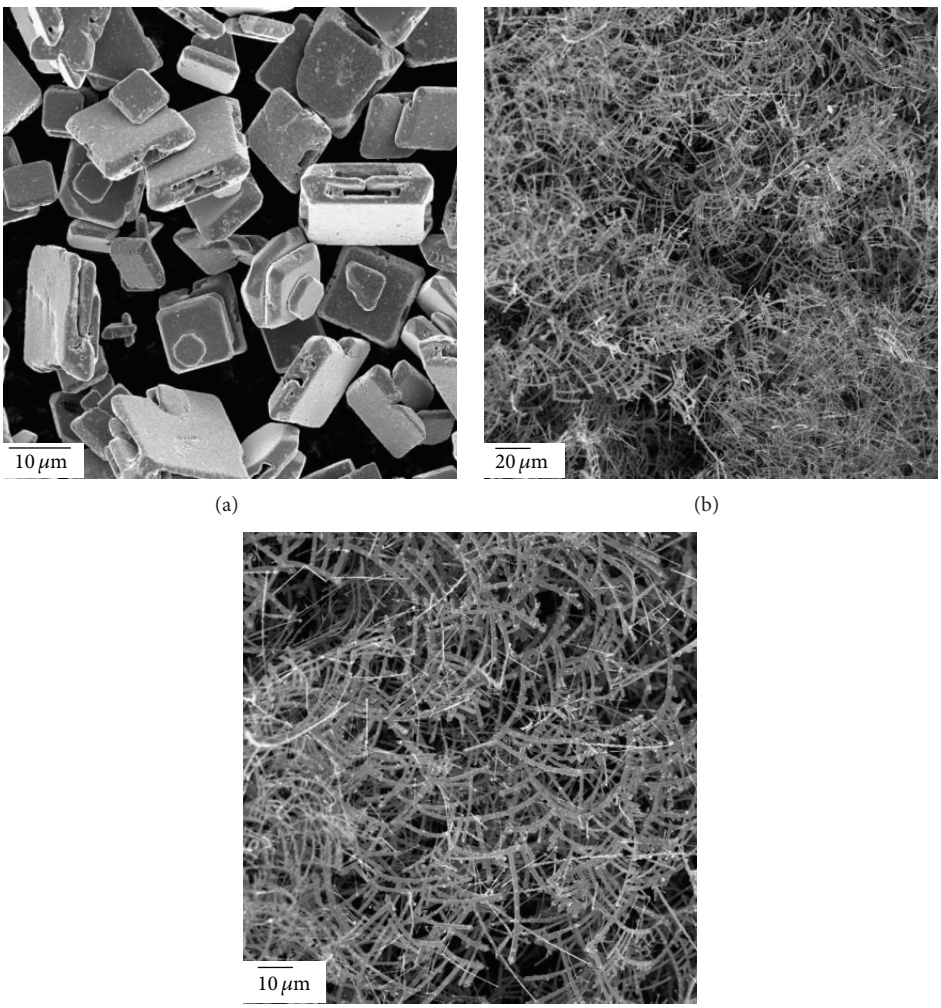

(a) (b) (c)

FIGURE 2: SEM micrographs of (a) pure commercially bought SnO powders and (b) and (c) SnO_2 nanowire networks synthesized at 1050°C for 30 min.

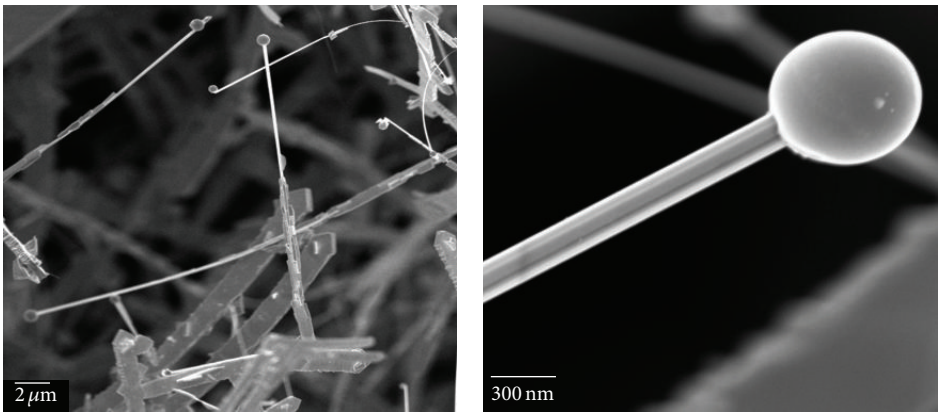

Figure 3: (a) SEM images of the synthesized SnO_2 nanowires and (b) a high magnification image of a single nanowire with a tip.

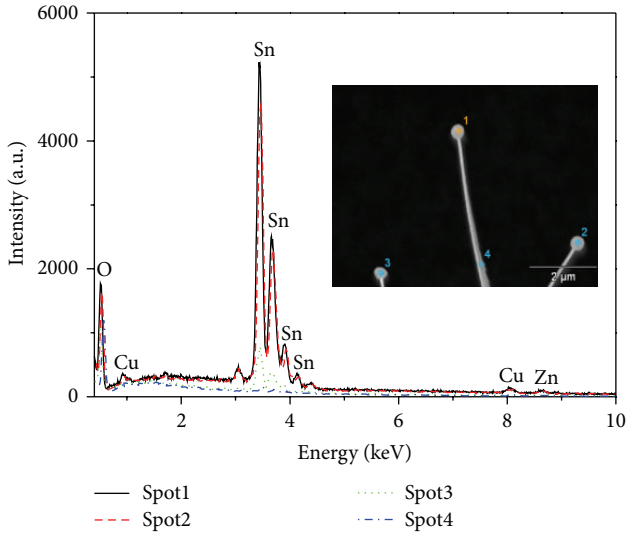

Figure 4: EDS spectra of four different spots of tin oxide nanowires. The inset shows the SEM images and the different spots analyzed.

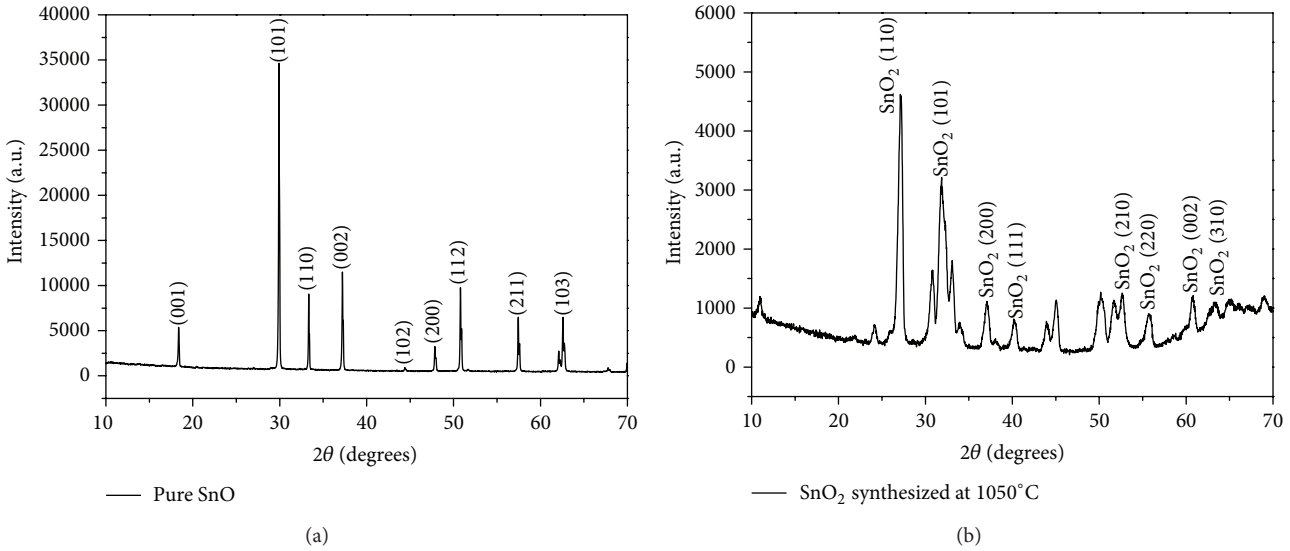

Figure 5: X-ray diffraction patterns of (a) pure SnO and (b) the as-synthesized SnO_2 nanowires at a growth temperature of 1050°C for 30 min.

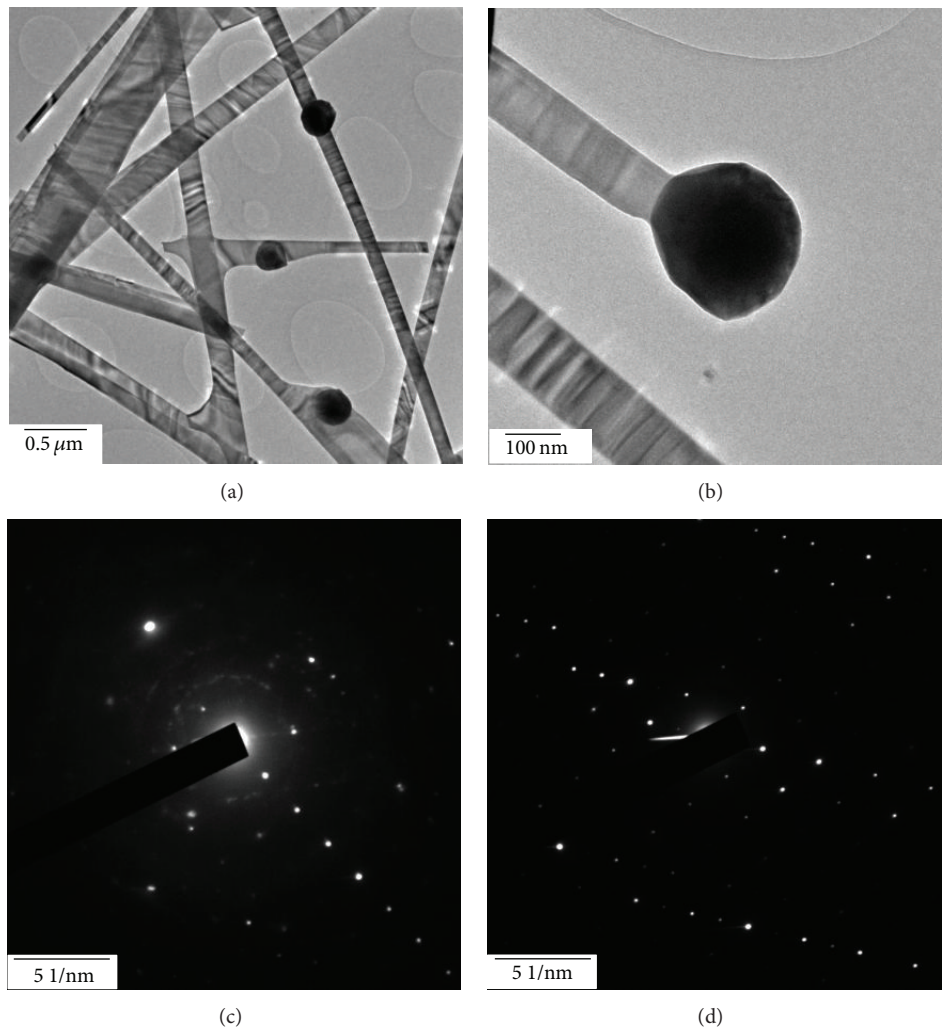

Figure 6: (a) and (b) Bright-field TEM images of SnO_2 nanowires and the corresponding diffraction patterns of (c) tip and (d) tail of the nanowires.

energy, growth direction, and diameter of the final 1D metal oxide nanostructures. Briefly, the following chemical reaction will take place during the thermal evaporation process [29]:

$$2\mathrm{SnO}\,(\mathrm{g}) \longrightarrow \mathrm{Sn}\,(\mathrm{l}) + \mathrm{SnO_2}\,(\mathrm{s})\,. \quad (2)$$

It is believed that tin oxide (SnO) vapor will be transferred by the argon gas (Ar) or is naturally spread out by thermal diffusion to the deposition area. Because SnO is metastable, it will decompose into Sn and SnO_2 above 600°C, forming Sn droplets as shown from the previous equation. According to this mechanism, a metal catalyst is needed for Sn-metal alloy droplets by the reaction with the metal catalyst particles. At the same time, these droplets can provide the energetically favored sites for adsorption of SnO vapor. Subsequently, the decomposition of SnO will result in the precipitation of SnO_2, and this leads to the formation of SnO_2 nanostructures [32]. However, in this process, no catalyst was used, and therefore the growth of the nanowires is not consistent with the VLS model but governed by the VS mechanism. Therefore, the nanonuclei necessary for the VLS growth of nanowires, which used to be obtained by adding an adscititious metal catalyst, can also be created through internal chemical reactions of precursors which are considered to be a self-catalytic growth, which is in good agreement with the results obtained by the EDS analysis.

4. Conclusions

SnO_2 nanowires have been successfully synthesized using a quartz tube-based CVD reactor at a growth temperature of 1050°C for 30 minutes. The microstructures and surface compositions of the nanowires were characterized by SEM-EDS, XRD, and TEM. The SEM micrographs revealed "wool-like" structures with a network of nanowires, ribbons, and belts. The nanowires follow the vapor-liquid-solid growth mechanism which is evident because of the liquid droplets on the tip of the nanowires. They serve as transporting medium as the nanowires develop as a result of the precipitation process. No metal catalyst was used in the synthesis of these nano wires which proves that the tin oxide is self-catalytic during the synthesis process. EDX analysis showed

that the samples are purely Sn and O with a 1 : 2 weight ratio. Nanowires have diameters in the range of 50–200 nm and length 10–100 μm. X-ray diffraction analysis confirmed that the as-synthesized materials are highly crystalline. The band gap value of the SnO_2 nanowires obtained by UV-vis was around 3.7 eV.

Acknowledgments

The authors would like to acknowledge the financial support of the Council for Scientific and Industrial Research (CSIR), South Africa, (Project no.: HGER27S) and the Department of Science and Technology.

References

[1] S. Y. Li, C. Y. Lee, and T. Y. Tseng, "Copper-catalyzed ZnO nanowires on silicon (1 0 0) grown by vapor-liquid-solid process," *Journal of Crystal Growth*, vol. 247, no. 3-4, pp. 357–362, 2003.

[2] J. X. Wang, D. F. Liu, X. Q. Yan et al., "Growth of SnO_2 nanowires with uniform branched structures," *Solid State Communications*, vol. 130, no. 1-2, pp. 89–94, 2004.

[3] Z. W. Pan, Z. R. Dai, L. Xu, S. T. Lee, and Z. L. Wang, "Temperature-controlled growth of silicon-based nanostructures by thermal evaporation of SiO powders," *Journal of Physical Chemistry B*, vol. 105, no. 13, pp. 2507–2514, 2001.

[4] K. D. Schierbaum, U. Weimar, and W. Gopel, "Schottky-barrier and conductivity gas sensors based upon Pd/SnO_2 and Pt/TiO_2," *Sensors and Actuators B*, vol. 4, no. 1-2, pp. 87–94, 1992.

[5] D. E. Williams, "Semiconducting oxides as gas-sensitive resistors," *Sensors and Actuators B*, vol. 57, no. 1–3, pp. 1–16, 1999.

[6] W. Fliegel, G. Behr, J. Werner, and G. Krabbes, "Preparation, development of microstructure, electrical and gas-sensitive properties of pure and doped SnO_2 powders," *Sensors and Actuators B*, vol. 19, no. 1–3, pp. 474–477, 1994.

[7] G. Korotcenkov, "Metal oxides for solid-state gas sensors: what determines our choice?" *Materials Science and Engineering: B*, vol. 139, no. 1, pp. 1–23, 2007.

[8] G. Korotcenkov, V. Brynzari, and S. Dmitriev, "SnO_2 films for thin film gas sensor design," *Materials Science and Engineering: B*, vol. 63, no. 3, pp. 195–204, 1999.

[9] N. Yamazoe, Y. Kurokawa, and T. Seiyama, "Effects of additives on semiconductor gas sensors," *Sensors and Actuators*, vol. 4, pp. 283–289, 1983.

[10] G. Zhang and M. Liu, "Effect of particle size and dopant on properties of SnO_2-based gas sensors," *Sensors and Actuators B*, vol. 69, no. 1, pp. 144–152, 2000.

[11] K. J. Albert, N. S. Lewis, C. L. Schauer et al., "Cross-reactive chemical sensor arrays," *Chemical Reviews*, vol. 100, no. 7, pp. 2595–2626, 2000.

[12] M. Meyyappan and M. S. Sunkara, *Inorganic Nanowires*, CRC, Boca Raton, Fla, USA, 2009.

[13] Z. Ying, Q. Wan, Z. T. Song, and S. L. Feng, "SnO_2 nanowhiskers and their ethanol sensing characteristics," *Nanotechnology*, vol. 15, no. 11, pp. 1682–1684, 2004.

[14] V. V. Sysoev, B. K. Button, K. Wepsiec, S. Dmitriev, and A. Kolmakov, "Toward the nanoscopic "electronic nose": hydrogen vs carbon monoxide discrimination with an array of individual metal oxide nano- and mesowire sensors," *Nano Letters*, vol. 6, no. 8, pp. 1584–1588, 2006.

[15] J. G. Lu, P. Chang, and Z. Fan, "Quasi-one-dimensional metal oxide materials—synthesis, properties and applications," *Materials Science and Engineering: R*, vol. 52, no. 1–3, pp. 49–91, 2006.

[16] N.-L. Wu, S.-Y. Wang, and I. A. Rusakova, "Inhibition of crystallite growth in the sol-gel synthesis of nanocrystalline metal oxides," *Science*, vol. 285, no. 5432, pp. 1375–1377, 1999.

[17] Y. Wang, X. Jiang, and Y. Xia, "A solution-phase, precursor route to polycrystalline SnO_2 nanowires that can be used for gas sensing under ambient conditions," *Journal of the American Chemical Society*, vol. 125, no. 52, pp. 16176–16177, 2003.

[18] M. Yuasa, T. Masaki, T. Kida, K. Shimanoe, and N. Yamazoe, "Nano-sized PdO loaded SnO_2 nanoparticles by reverse micelle method for highly sensitive CO gas sensor," *Sensors and Actuators B*, vol. 136, no. 1, pp. 99–104, 2009.

[19] M. H. Huang, Y. Wu, H. Feick, N. Tran, E. Weber, and P. Yang, "Catalytic growth of zinc oxide nanowires by vapor transport," *Advanced Materials*, vol. 13, no. 2, pp. 113–116, 2001.

[20] J. D. Holmes, K. P. Johnston, R. C. Doty, and B. A. Korgel, "Control of thickness and orientation of solution-grown silicon nanowires," *Science*, vol. 287, no. 5457, pp. 1471–1473, 2000.

[21] J. S. Jeong, J. Y. Lee, C. J. Lee, S. J. An, and G. C. Yi, "Synthesis and characterization of high-quality In_2O_3 nanobelts via catalyst-free growth using a simple physical vapor deposition at low temperature," *Chemical Physics Letters*, vol. 384, no. 4–6, pp. 246–250, 2004.

[22] M. J. Zheng, L. D. Zhang, G. H. Li, X. Y. Zhang, and X. F. Wang, "Ordered indium-oxide nanowire arrays and their photoluminescence properties," *Applied Physics Letters*, vol. 79, p. 839, 2001.

[23] N. G. Patel, K. K. Makhija, C. J. Panchal, D. B. Dave, and V. S. Vaishnav, "Fabrication of carbon tetrachloride gas sensors using indium tin oxide thin films," *Sensors and Actuators B*, vol. 23, no. 1, pp. 49–53, 1995.

[24] D. Frohlich and R. Kenklies, "Band-gap assignment in SnO_2 by two-photon spectroscopy," *Physical Review Letters*, vol. 41, no. 25, pp. 1750–1751, 1978.

[25] G. Mill, Z. G. Li, and D. Merisel, "Photochemistry and spectroscopy of colloidal arsenic sesquisulfide," *The Journal of Physical Chemistry*, vol. 92, no. 3, pp. 822–828, 1988.

[26] S. Luo, P. K. Chu, W. Liu, M. Zhang, and C. Lin, "Origin of low-temperature photoluminescence from SnO_2 nanowires fabricated by thermal evaporation and annealed in different ambients," *Applied Physics Letters*, vol. 88, Article ID 183112, 3 pages, 2006.

[27] A. L. Efros and A. L. Efros, "Interband absorption of light in a semiconductor sphere," *Soviet Physics: Semiconductors*, vol. 16, pp. 772–775, 1982.

[28] L. Brus, "A simple model for the ionization potential, electron affinity, and aqueous redox potentials of small semiconductor crystallites," *Journal of Chemical Physics*, vol. 79, no. 11, p. 5566, 1983.

[29] B. Wang, Y. H. Yang, C. X. Wang, and G. W. Yang, "Nanostructures and self-catalyzed growth of SnO_2," *Journal of Applied Physics*, vol. 98, no. 7, Article ID 073520, 5 pages, 2005.

[30] R. S. Wagner and W. C. Ellis, "Vapor-liquid-solid mechanism of single crystal growth," *Applied Physics Letters*, vol. 4, no. 5, p. 89, 1964.

[31] G. Gundiah, A. Govindaraj, and C. N. R. Rao, "Nanowires, nanobelts and related nanostructures of Ga_2O_3," *Chemical Physics Letters*, vol. 351, no. 3-4, pp. 189–194, 2002.

[32] A. Kolmakov, Y. Zhang, G. Cheng, and M. Moskovits, "Detection of CO and O_2 using tin oxide nanowire sensors," *Advanced Materials*, vol. 15, no. 12, pp. 997–1000, 2003.